

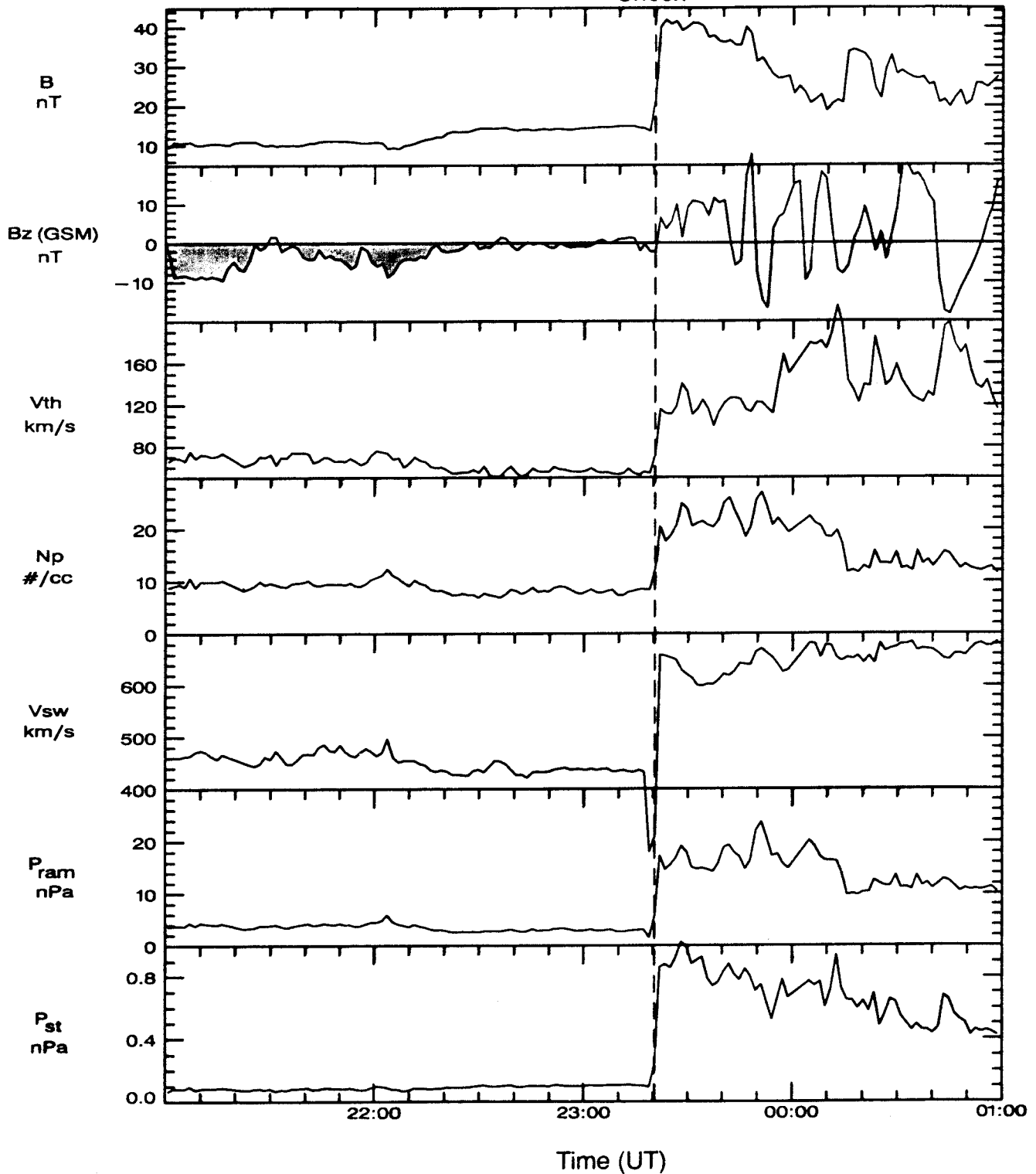
INTERPLANETARY SHOCK TRIGGERING OF AURORAL SUBSTORM ACTIVITY: A MECHANISM

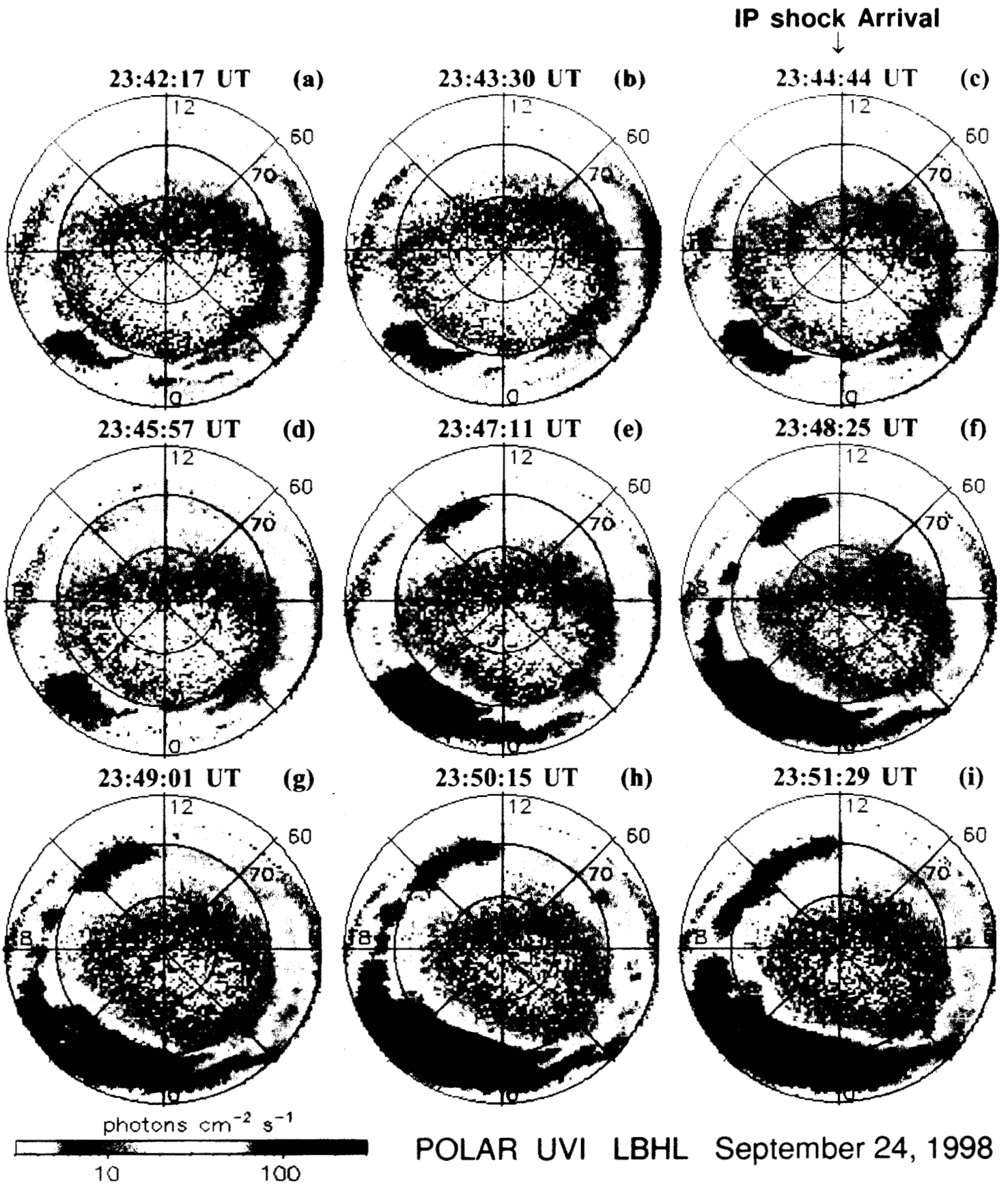
B. T. Tsurutani (1), X.-Y. Zhou (1), J. K. Arballo (1) and G. S. Lakhina (2)
(1) Jet Propulsion Laboratory, Pasadena, California. (2) Indian Institute of
Geomagnetism, Colaba, Mumbai/Bombay, India.

btsurutani@jplsp2.jpl.nasa.gov

We use 1997-1998 WIND solar wind data and POLAR UV imaging data to study magnetospheric responses and substorm triggering mechanisms during and after interplanetary (IP) shock events. The nightside auroral responses are classified into three types: substorm expansion phase (SS) (or substorm further intensification) events, pseudobreakup (PB) events, and quiescent (QE) events. It is found that the solar wind precondition determines the causes of the different auroral responses, with a ~ 1.5 hr "precondition" (upstream of the IP shock) giving the best empirical results. The upstream IMF B_z is strongly southward prior to substorm triggerings (44% of all events), the IMF B_z is ~ 0 nT for PB triggerings (39% of all events), and the IMF is almost purely northward for quiescent events (17%). A magnetotail-compression substorm triggering model is developed and presented. This model uses dayside magnetic reconnection to load the near-Earth plasma sheet and a current disruption mechanism to unload the stored energy. We call this model a Dripping, Tilting Bucket (DTB) model.

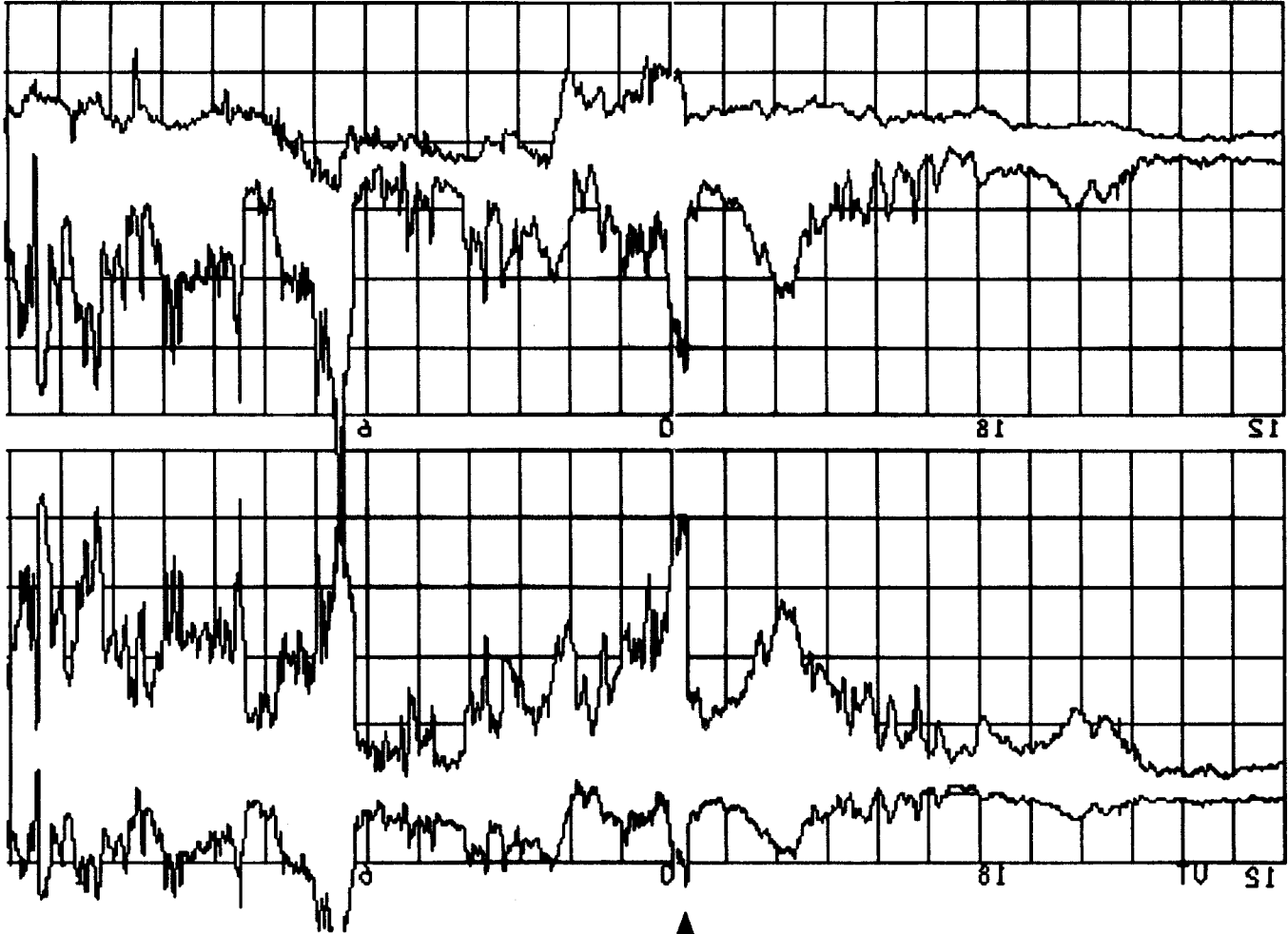
WIND - September 24, 1998
Shock





QUICK LOOK WDC-CS KYOTO

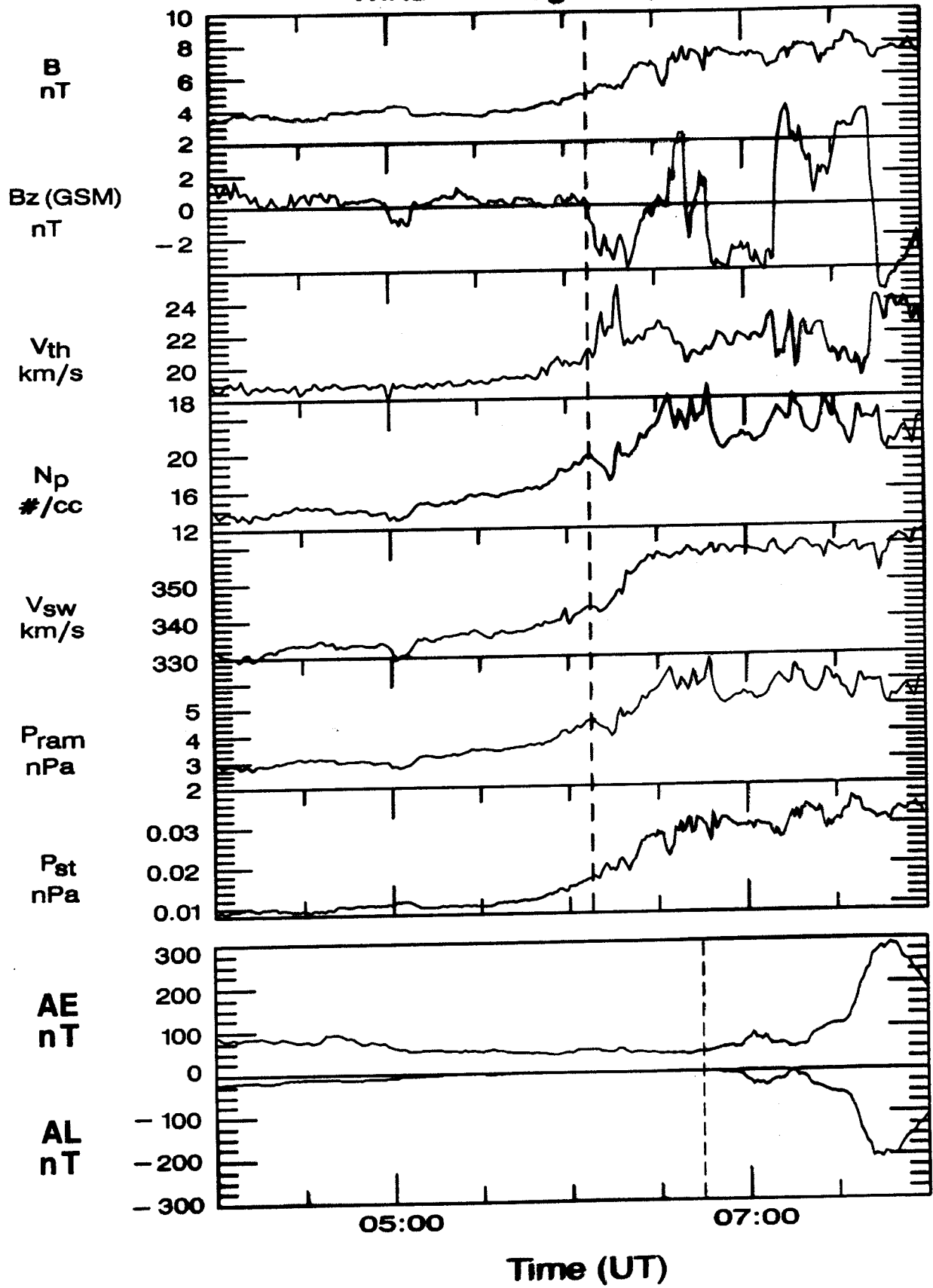
0154-52198 AE (8)



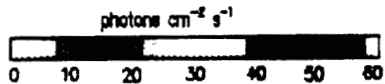
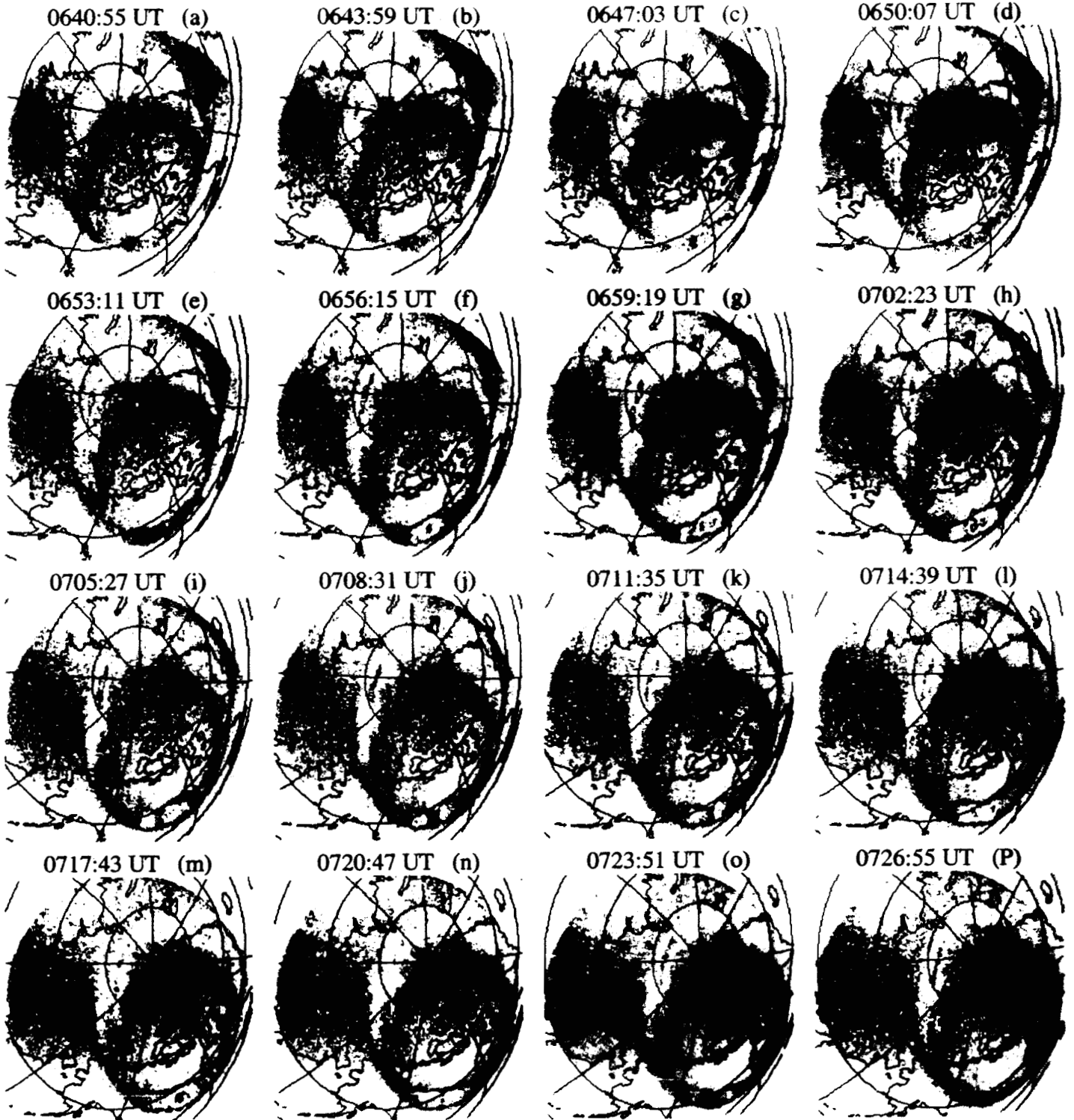
↑
substorm intensification IP shock triggered

after 2000 31/8 hour 21

WIND - August 9, 1997



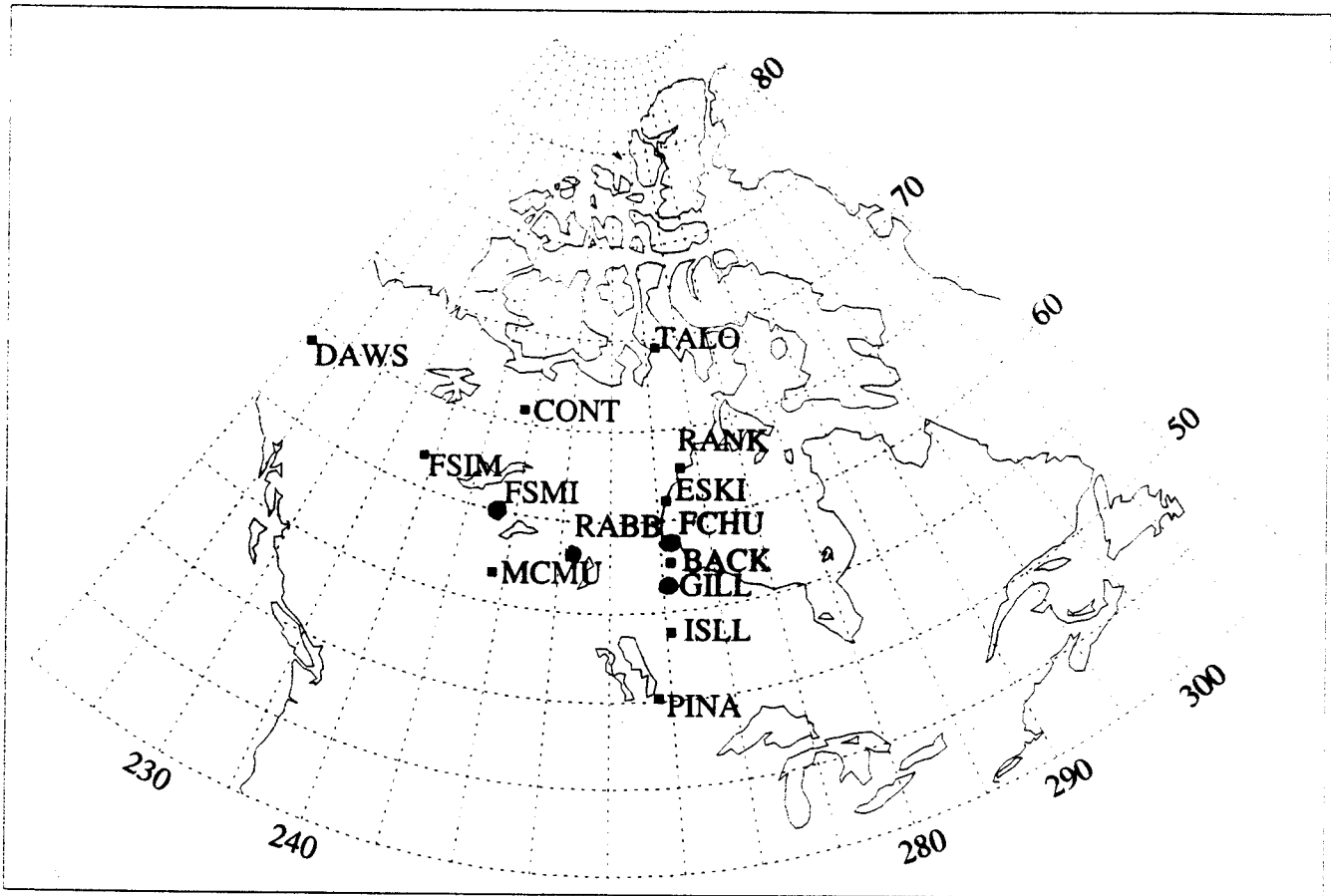
Pressure Pulse Arrival



POLAR UVI LBHS 36.8 s IP

August 9, 1997

(By courtesy of Dr. Terry Hughes of CANOPUS team)

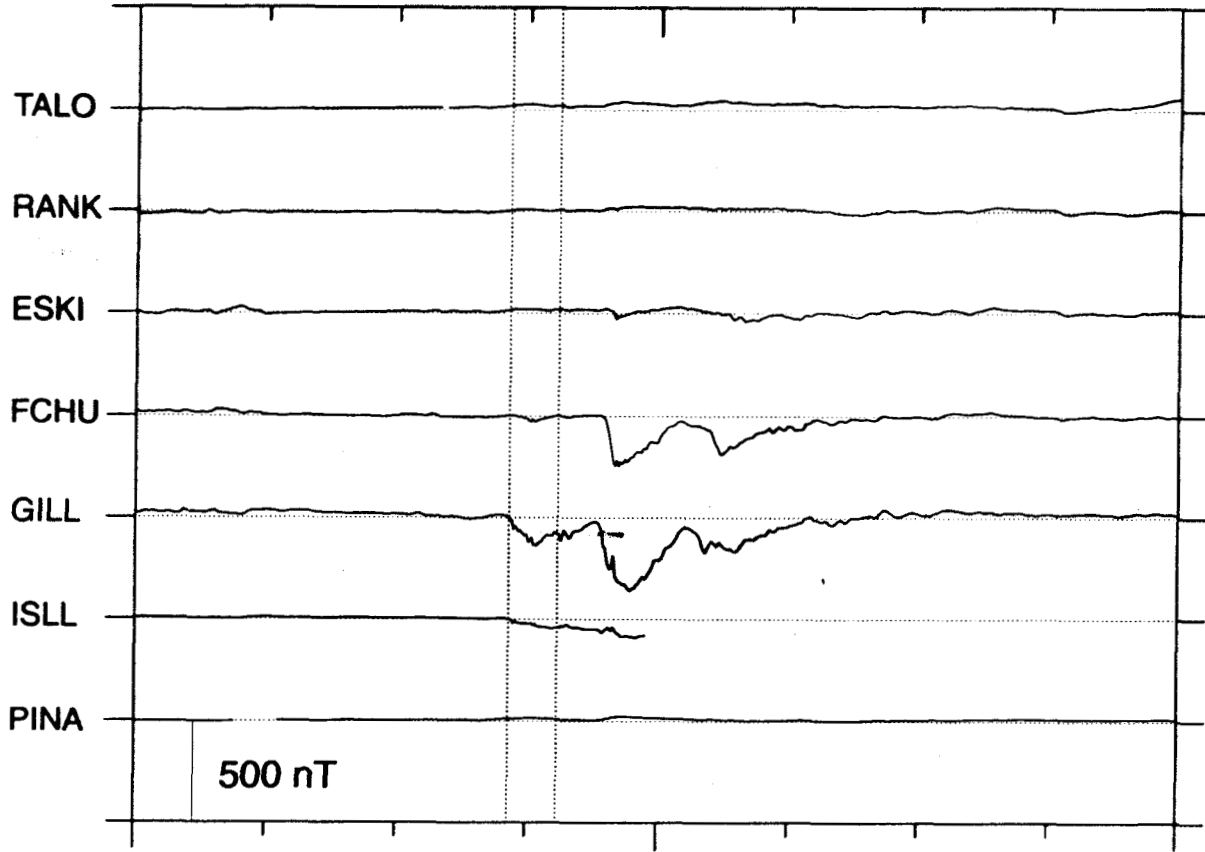


Magnetometer Site Coordinates

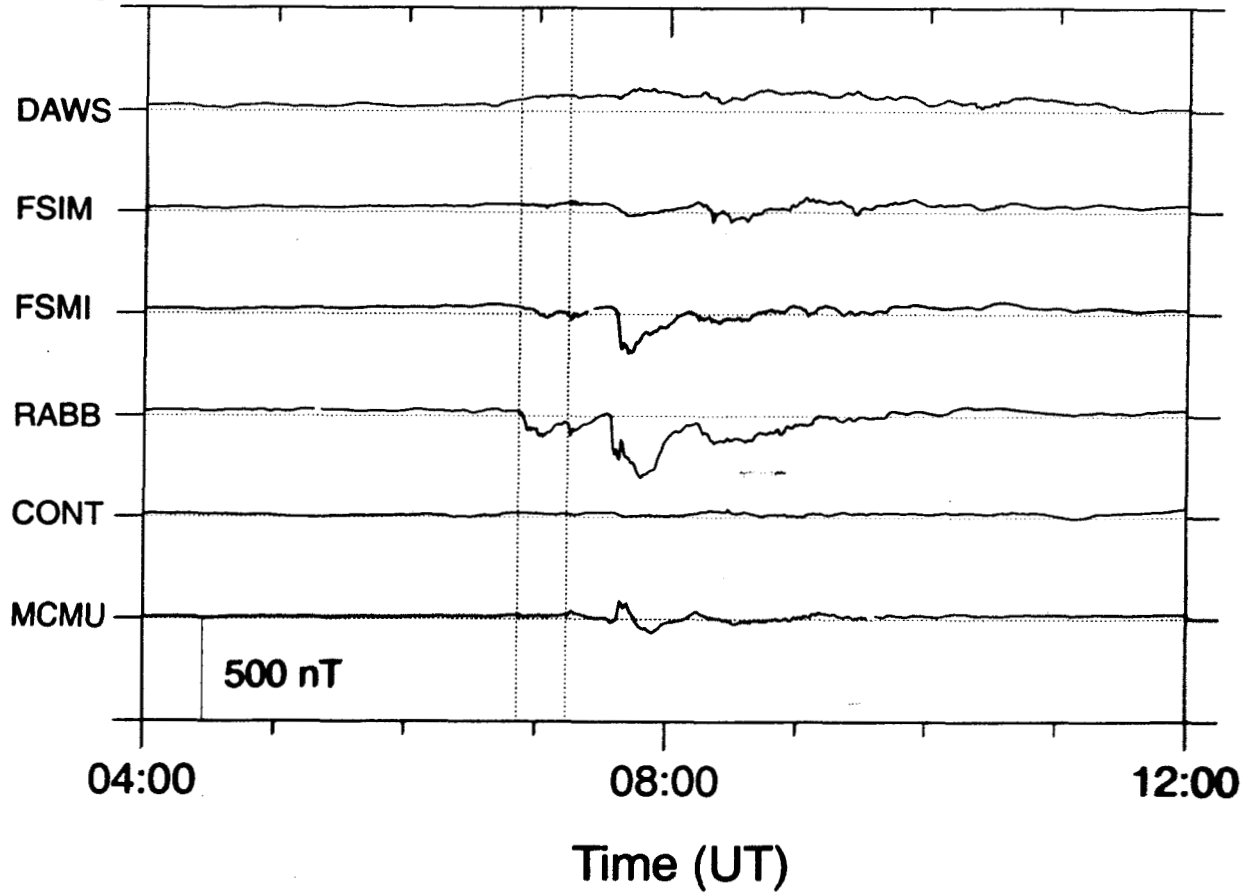
LOCATION	SITE CODE	GEODETIC LAT	GEODETIC LONG	CANOPUS EDFL ¹ LAT	CANOPUS EDFL ¹ LONG	L	INVLAT
Back	BACK	57.72	265.83	65.229	336.671	7.47	68.53
Contwoyto Lake	CONT	65.75	248.75	72.394	311.295	12.36	73.47
Dawson	DAWS	64.05	220.89	67.323	277.477	5.89	65.67
Eskimo Point	ESKI	61.11	265.95	68.621	336.465	10.20	71.75
Fort Churchill	FCHU	58.76	265.92	66.268	336.682	8.18	69.53
Fort McMurray	MCMU	56.66	248.79	63.233	315.304	5.49	64.74
Fort Simpson	FSIM	61.76	238.77	67.396	300.580	6.84	67.52
Fort Smith	FSMI	60.02	248.05	66.556	313.205	7.05	67.88
Gillam	GILL	56.38	265.36	63.883	336.205	6.66	67.20
Island Lake	ISLL	53.86	265.34	61.385	336.419	5.49	64.74
Pinawa	PINA	50.20	263.96	57.732	335.079	4.25	60.98
Rabbit Lake	RABB	58.22	256.32	65.333	324.380	6.94	67.69
Rankin Inlet	RANK	62.82	267.89	70.374	338.923	12.44	73.53
Taloyoak	TALO	69.54	266.45	77.145	335.856	29.96	79.47

¹EDFL ==> Eccentric Dipole Field Line traced coordinates.

Meridional Chain 0652 UT 0714 UT

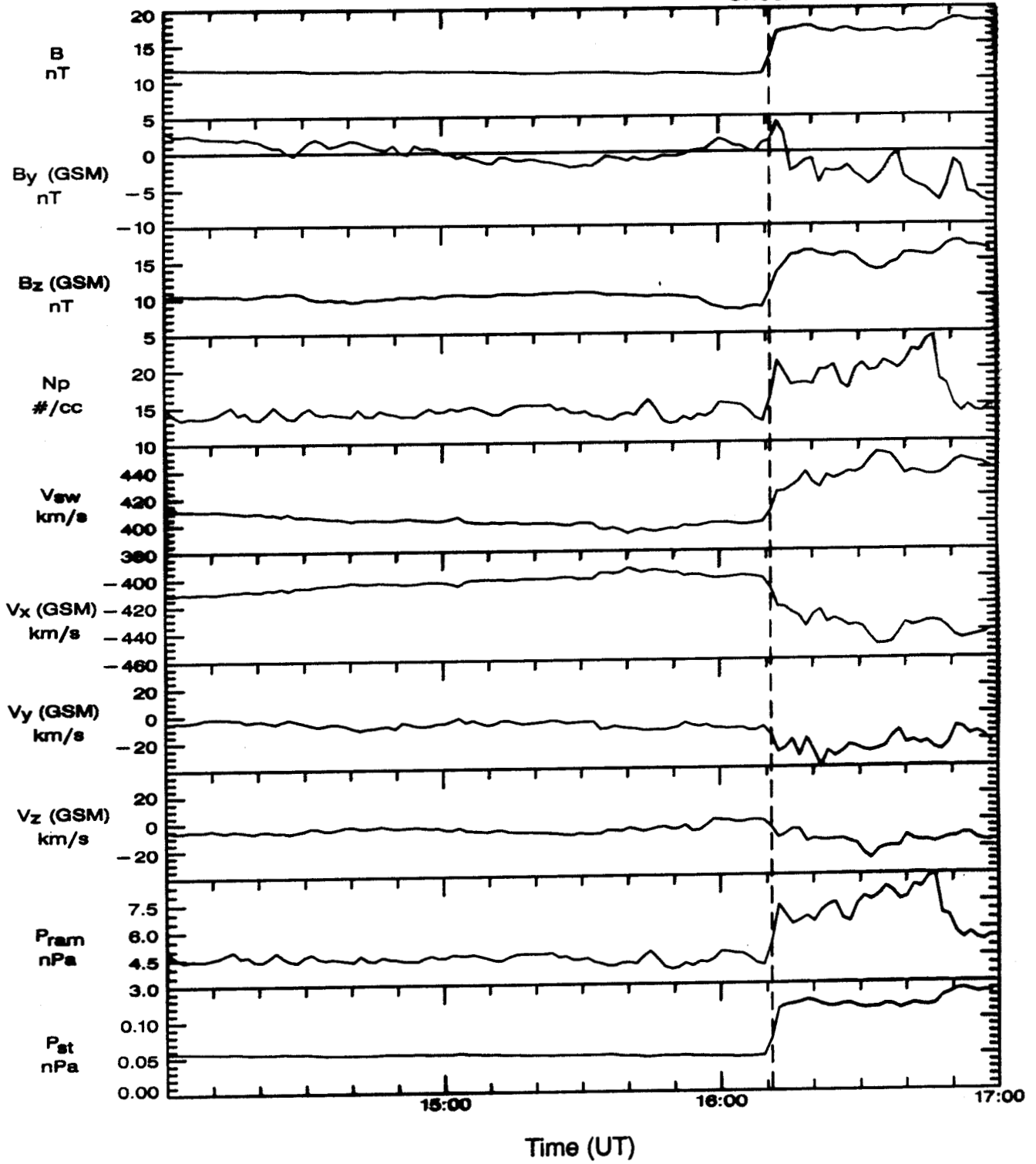


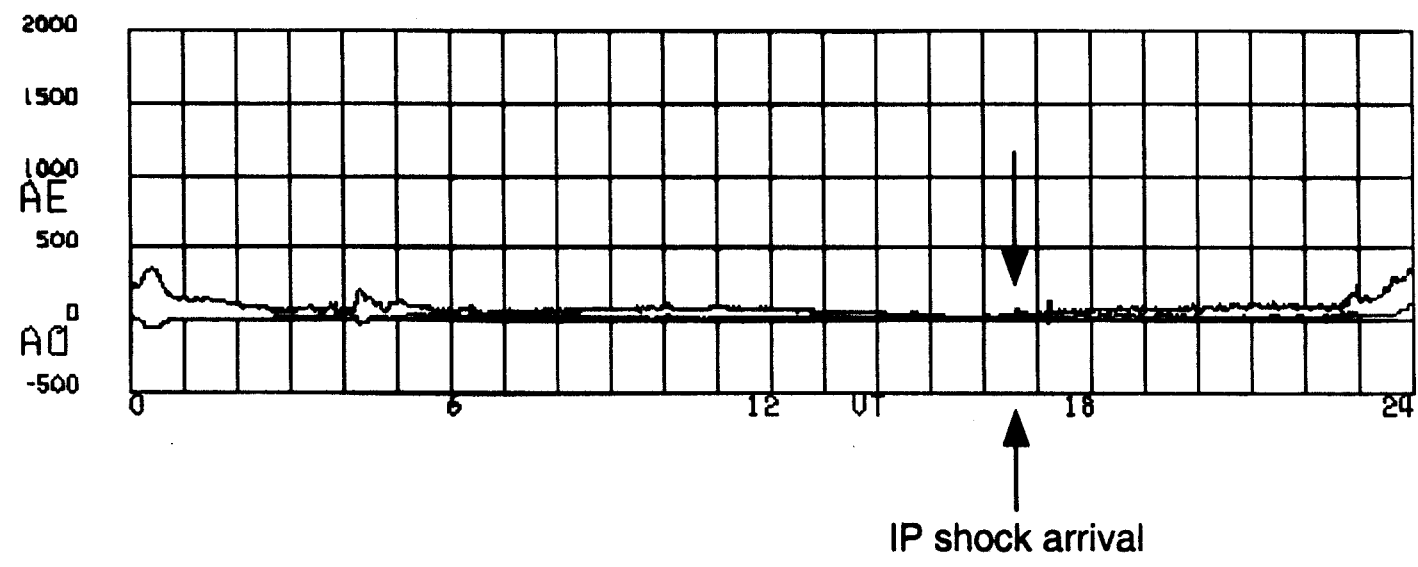
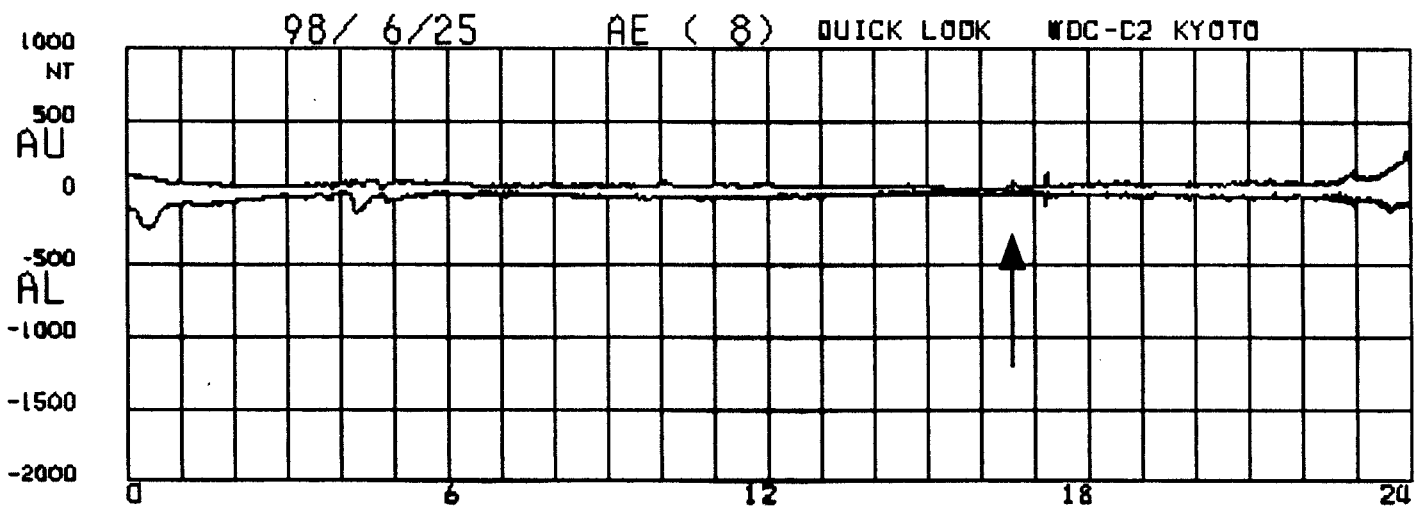
Longitudinal Chain



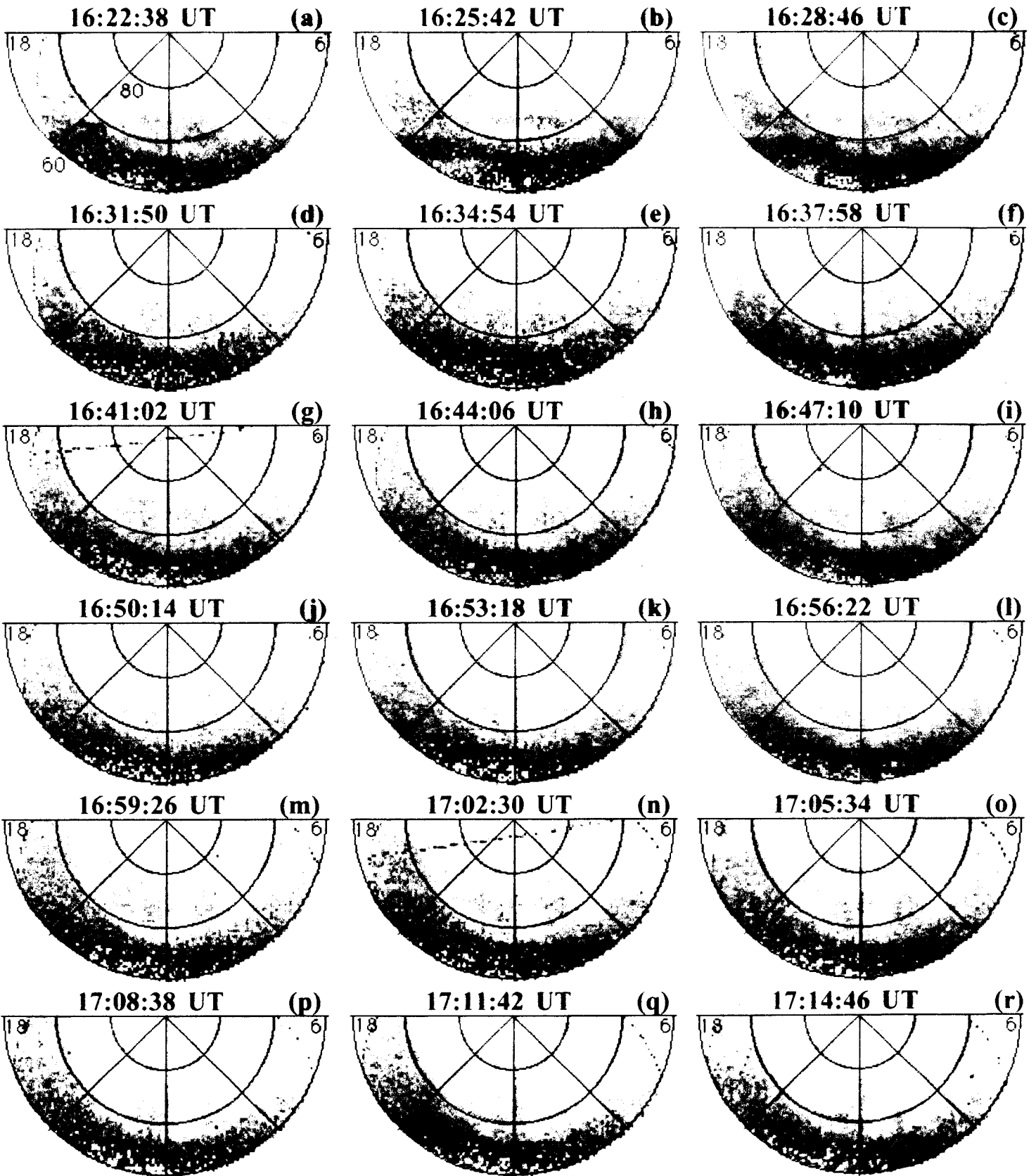
WIND - June 25, 1998

Shock

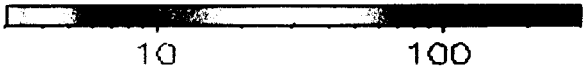




IP Shock Arrival



photons $\text{cm}^{-2} \text{s}^{-1}$



POLAR UVI LBHL

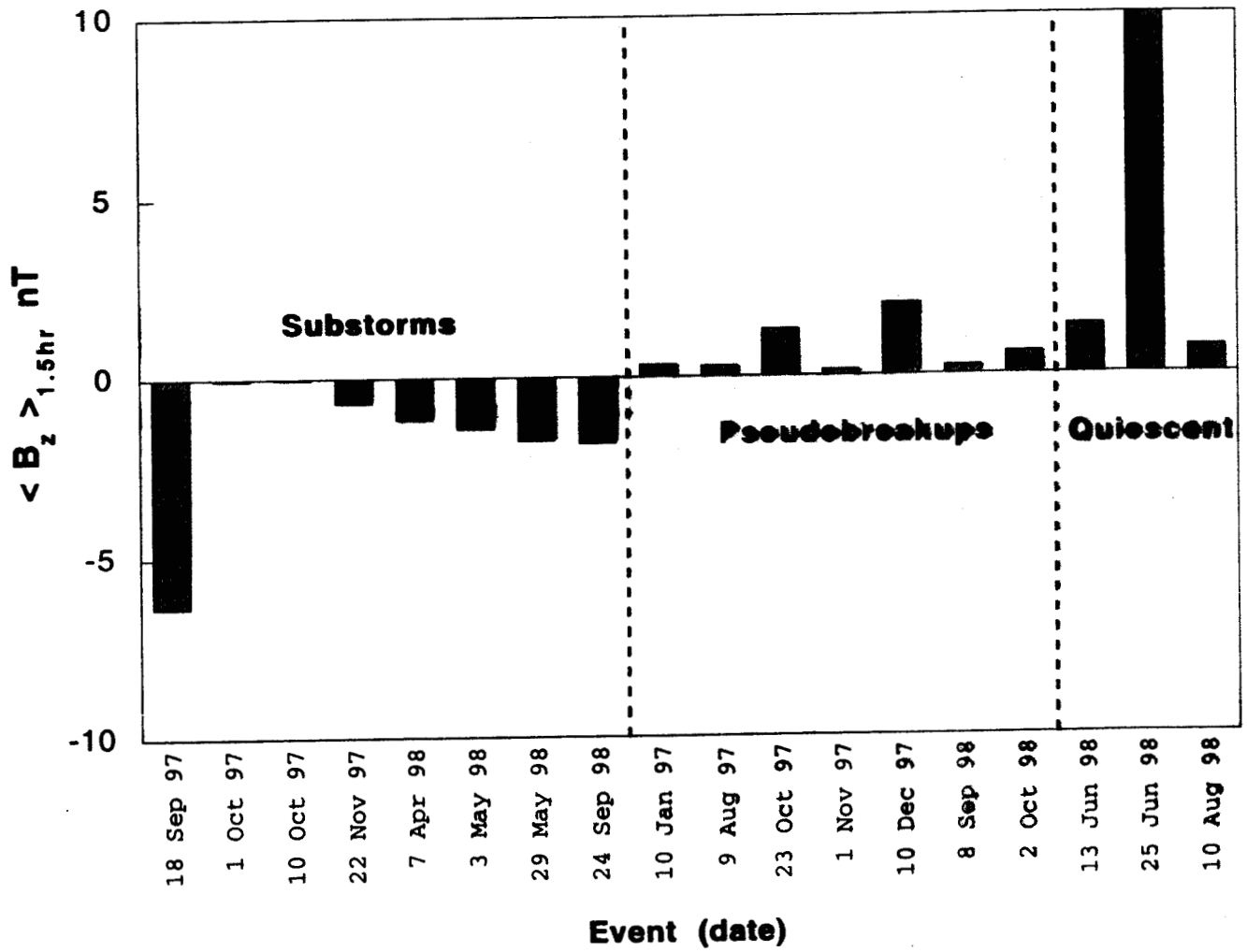
June 25, 1998

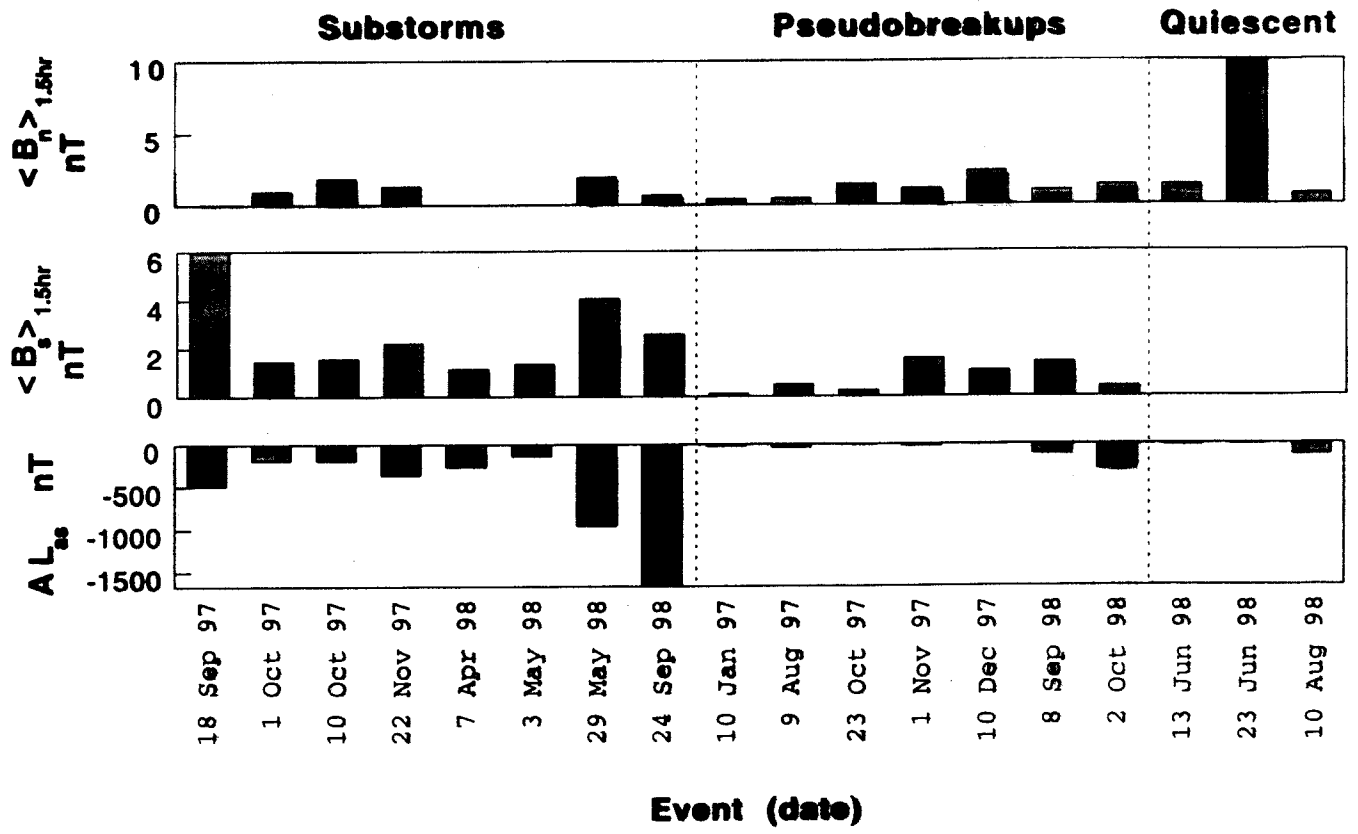
Table 1. Preconditions of 18 IP shock associated events

Type	Date	IMF \bar{B} (nT)	IMF \bar{B}_s (nT)	IMF \bar{B}_n (nT)	IMF \bar{B}_z (nT)	\bar{V}_{sw} (km/s)	\bar{N}_p (#/cc)	\bar{P}_{ram} (nPa)	\bar{P}_{st} (nPa $\times 10^{-3}$)	\overline{AL}_{ps} (nT)
SS	Sep 18, 1997	6.7	6.4	0.0	-6.4	331	12.2	3.5	20.3	-302
	Oct 1, 1997	3.5	1.5	0.9	-0.05	429	12.6	4.1	11.4	-68
	Oct 10, 1997	8.9	1.6	1.8	-0.03	414	11.8	4.5	34.6	-43
	Nov 22, 1997	6.4	2.3	1.3	-0.7	349	12.6	3.4	32.7	-37
	Apr 7, 1998	7.1	1.2	0.0	-1.2	293	10.4	2.0	23.0	-35
	May 3, 1998	3.2	1.4	0.0	-1.4	430	4.7	2.0	4.6	-32
	May 29, 1998	11.3	4.2	1.9	-1.7	518	8.8	5.3	90.4	-165
	Sep 24, 1998	12.3	2.7	0.7	-1.8	446	8.6	3.9	94.8	-498
PB	Jan 10, 1997	2.4	0.1	0.4	0.3	375	7.7	2.4	5.5	-5
	Aug 9, 1997	3.9	0.5	0.4	0.3	335	15.0	3.8	10.8	0
	Oct 23, 1997	5.0	0.3	1.4	1.3	300	7.5	1.5	14.9	-8
	Nov 1, 1997	6.0	1.6	1.1	0.1	341	30.7	8.0	21.9	-42
	Dec 10, 1997	6.2	1.1	2.4	2.0	286	11.0	2.0	19.6	-5
	Sep 8, 1998	9.0	1.5	1.0	0.2	328	4.7	1.1	33.0	-61
Oct 2, 1998	6.6	0.4	1.3	0.6	511	3.7	2.2	25.9	-22	
QE	Jun 13, 1998	4.6	0.0	1.4	1.4	315	3.4	0.8	9.0	3
	Jun 25, 1998	11.1	0.0	10.0	10.0	400	14.1	5.1	51.4	9
	Aug 10, 1998	4.9	0.0	0.7	0.7	400	4.8	1.7	11.0	-89

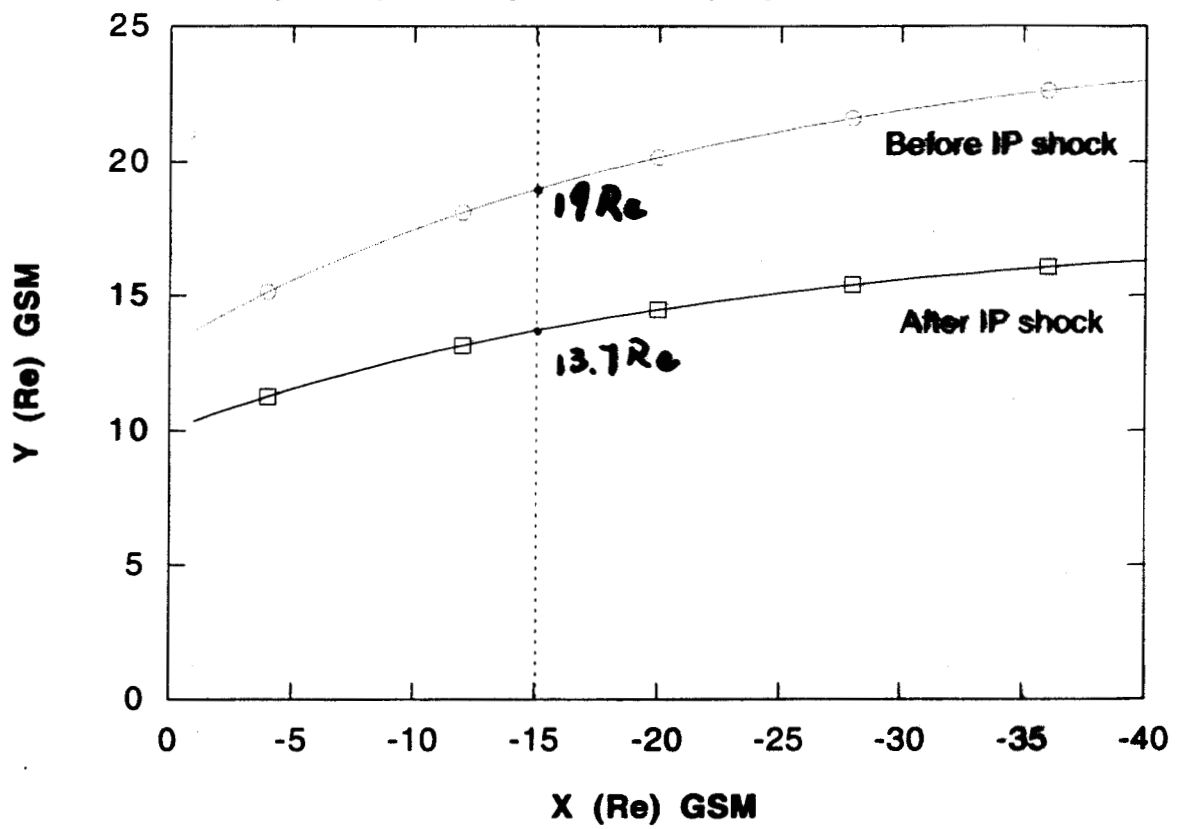
Table 2. Solar wind parameter variations at IP shocks and geomagnetic responses

Type	Date	IMF Bz (nT) Turning	$IMF(\Delta B/\bar{B})$	$(\Delta V/\bar{V})_{sw}$	$(\Delta N_p/N_p)$	$(\Delta P/\bar{P})_{rum}$	$(\Delta P/\bar{P})_{st}$	Delay T (min)	M Lat (°)	AL_{ur} Peak (nT)
SS	Sep 18, 1997	-6 to -9	0.4	0.07	0.4	0.4	0.9	6	66	-491
	Oct 1, 1997	-2 to 5	2.8	0.08	2.3	2.3	3.9	9	67	-185
	Oct 10, 1997	-0.5	0.6	0.07	0.7	0.7	1.4	10	65	-190
	Nov 22, 1997	0 to -5	1.4	0.29	1.7	3.1	7.3	6	65	-363
	Apr 7, 1998	-1 to -7	0.8	0.14	1.4	1.6	2.4	6	70	-263
	May 3, 1998	-2 to -6	1.3	0.15	1.2	3.2	5.1	9	65	-136
	May 29, 1998	6 to -10	0.7	0.26	9.5	1.8	2.5	5	69	-955
	Sep 24, 1998	-1 to 3	2.3	0.48	1.4	4.1	9.7	4	65	-1670
PB	Jan 10, 1997	1 to 4	1.6	0.11	1.0	1.4	5.5	19	70	-24
	Aug 9, 1997	1 to -6	0.7	0.07	0.4	0.4	0.9	12	67	-35
	Oct 23, 1997	4 to 7	1.3	0.13	0.3	0.6	2.0	13	71	-9
	Nov 1, 1997	2 to 5	0.6	0.04	0.5	0.6	1.1	12	71	-22
	Dec 10, 1997	-1 to -3	1.7	0.26	1.6	2.4	6.0	12	72	-4
	Sep 8, 1998	1 to -2	0.2	0.12	2.8	0.9	0.6	12-13	68	-111
	Oct 2, 1998	5 to -2	1.8	0.40	1.8	3.3	9.9	6	70	-299
QE	Jun 13, 1998	2 to 8	1.1	0.19	8.6	3.5	4.7	N/A	N/A	-15
	Jun 25, 1998	9 to 13	0.6	0.09	0.1	0.6	1.3	N/A	N/A	-9
	Aug 10, 1998	1 to -1	1.1	0.12	9.4	1.6	3.3	N/A	N/A	-123

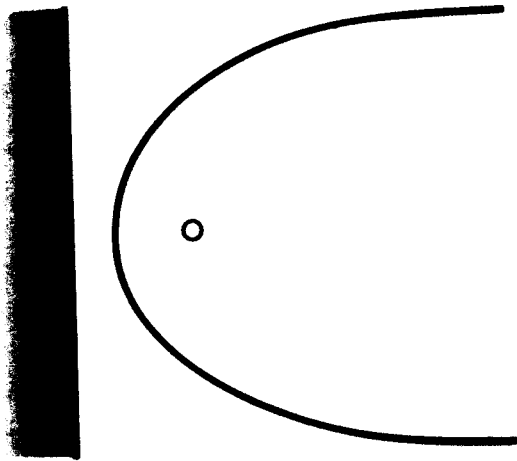




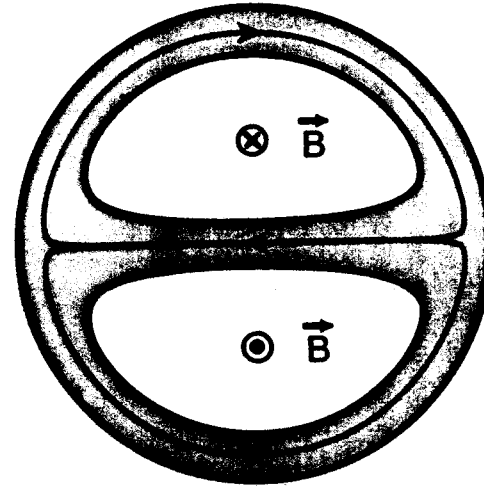
Magnetopause position (Sep 24, 1998 event)



Shock front

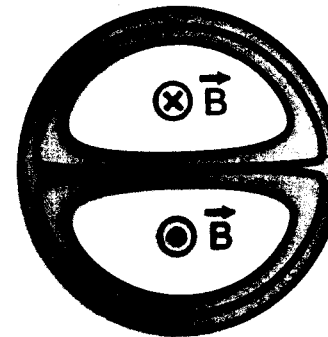
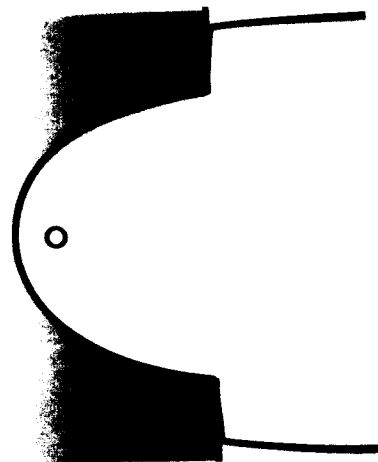


Magnetotail



(a)

Shock front



(b)

September 24, 1998 event

R: 19 ⇒ 13.3 Re (*at X = -15 Re*)

B_L ⇒ 2.1 B_L *I ⇒ 2.1 I (mA /m)*

P_L ⇒ 4.4 P_L *h ⇒ h/1.7* (*PV^γ*)_{CS} = *const.*

V_y ⇒ const. *E_y ⇒ 1.43 E_y*

For the ion Weibel instability, with certain simplicity the growth rate γ of the unstable wave is (Lui et al., JGR, 96, 11389, 1991)

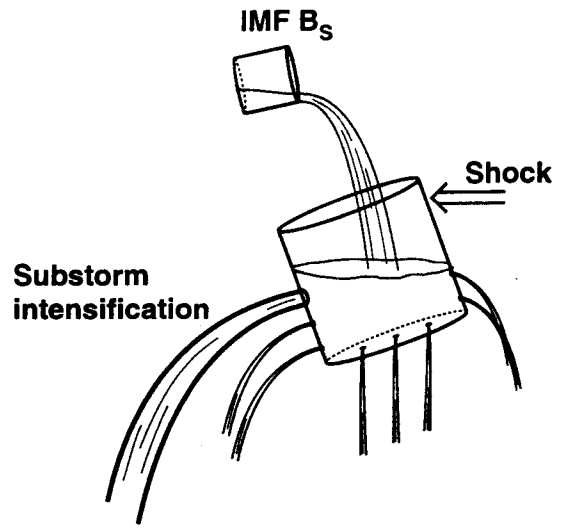
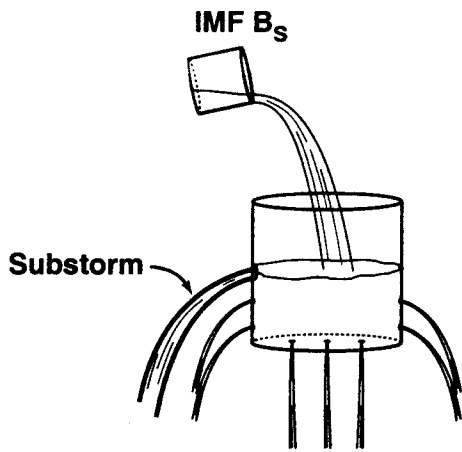
$$\gamma = \omega_{pi} V_0 / c$$

where ω_{pi} is the ion plasma frequency,
 V_0 is the ion drift speed along the E_y direction.

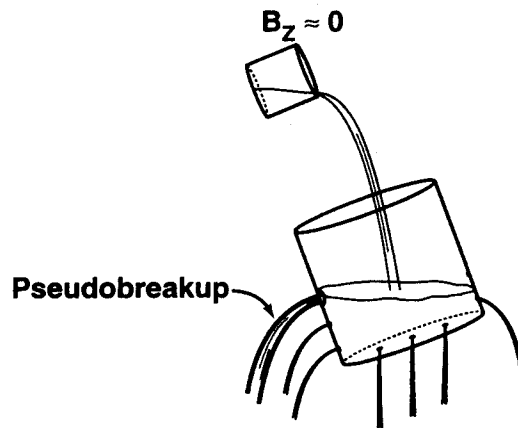
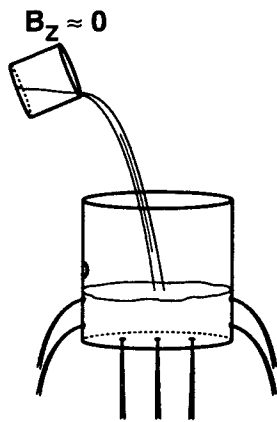
During southward IMF, when the plasma density = 6.0 cm^{-3} ,
the current sheet disruption can occur when $V_0 > 170 \text{ km/s}$.

During northward IMF, when the plasma density = 0.5 cm^{-3} ,
the current sheet disruption can occur when $V_0 > 600 \text{ km/s}$.

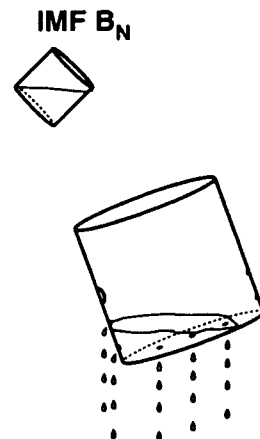
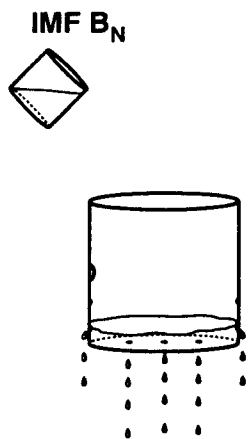
Dripping, Tilting Bucket Model



a)



b)



c)

SUMMARY AND CONCLUSIONS

1. IP shocks/pressure pulses can cause SSs, PBs or QE events. SS events are led by IMF B_z (precursors), PB events by IMF $B_z \approx 0$ and QE events by IMF B_n .
2. Compression of the near-Earth tail leads to an enhancement of the cross-tail current density (by 2.1 times), and an increase in E_y (by 1.43 times).
3. We have developed a Dripping, Tilting Bucket model which can explain all of the data reasonably well.
4. We therefore expect the substorm triggering signature in the near-Earth tail to be large, clear and fast. Thus by studying IP shock events, the mechanism for general substorm expansion onsets may be revealed.